Journal of Biomedical Optics

BiomedicalOptics.SPIEDigitalLibrary.org

Poly(3-hydroxybutyrate) anabolism in *Cupriavidus necator* cultivated at various carbon-to-nitrogen ratios: insights from single-cell Raman spectroscopy

Zhanhua Tao
Pengfei Zhang
Zhaojun Qin
Yong-Qing Li
Guiwen Wang

Zhanhua Tao, Pengfei Zhang, Zhaojun Qin, Yong-Qing Li, Guiwen Wang, "Poly(3-hydroxybutyrate) anabolism in *Cupriavidus necator* cultivated at various carbon-to-nitrogen ratios: insights from single-cell Raman spectroscopy," *J. Biomed. Opt.* **21**(9), 097005 (2016), doi: 10.1117/1.JBO.21.9.097005.

SPIE.

Poly(3-hydroxybutyrate) anabolism in *Cupriavidus necator* cultivated at various carbon-to-nitrogen ratios: insights from single-cell Raman spectroscopy

Zhanhua Tao,[a] Pengfei Zhang,[b] Zhaojun Qin,[a] Yong-Qing Li,[c] and Guiwen Wang[a,*]
[a]Guangxi Academy of Sciences, Laboratory of Biophysics, 98 Daling Road, Nanning, Guangxi 530007, China
[b]Washington University in St. Louis, Department of Biomedical Engineering, Optical Imaging Laboratory, One Brookings Drive, Campus Box 1097, St. Louis, Missouri 63130, United States
[c]East Carolina University, Department of Physics, East 5th Street, Greenville, North Carolina 27858, United States

Abstract. *Cupriavidus necator* accumulates large amounts of poly(3-hydroxybutyrate) (PHB), a biodegradable substitute for petroleum-based plastics, under certain nutrient conditions. Conventional solvent-extraction-based methods for PHB quantification only obtain average information from cell populations and, thus, mask the heterogeneity among individual cells. Laser tweezers Raman spectroscopy (LTRS) was used to monitor dynamic changes in the contents of PHB, nucleic acids, and proteins in *C. necator* at the population and single-cell levels when the microorganism cells were cultivated at various carbon-to-nitrogen ratios. The biosynthetic activities of nucleic acids and proteins were maintained at high levels, and only a small amount of PHB was produced when the bacterial cells were cultured under balanced growth conditions. By contrast, the syntheses of nucleic acids and proteins were blocked, and PHB was accumulated in massive amount inside the microbial cells under nitrogen-limiting growth circumstances. Single-cell analysis revealed a relatively high heterogeneity in PHB level at the early stage of the bacterial growth. Additionally, bacterial cells in populations at certain cultivation stages were composed of two or three subpopulations on the basis of their PHB abundance. Overall, LTRS is a reliable single-cell analysis tool that can provide insights into PHB fermentation. [DOI: 10.1117/1.JBO.21.9.097005]

Keywords: Raman spectroscopy; laser tweezers; poly(3-hydroxybutyrate); Cupriavidus necator.

Paper 160485R received Jul. 13, 2016; accepted for publication Aug. 24, 2016; published online Sep. 16, 2016.

1 Introduction

Polyhydroxyalkanoates (PHAs) have drawn considerable attention as biodegradable substitutes for conventional petroleum-based plastics because of their similar material properties to various thermoplastics and elastomers, and complete biodegradability under various environments.[1] Poly(3-hydroxybutyrate) (PHB), the most common PHA, is an intracellular carbon and energy storage material found in diverse bacteria. PHB is usually produced and accumulated when the carbon source is in excess but another essential element, such as N, P, Mg, K, O, or S, is limited.[2] The accumulated PHB is degraded and reused once carbon sources are exhausted.

To commercialize PHB, the production cost of this polymer must first be reduced. This goal may be achieved by developing suitable bacterial strains and an efficient fermentation process. *Cupriavidus necator* (formerly known as *Ralstonia eutropha* or *Alcaligenes eutrophus*), which is widely used to produce PHB, can accumulate PHB in amounts reaching 80% to 90% of dry cell weight when fructose was used as a carbon source and the nitrogen source supply was limited.[3] Environmental factors substantially affect PHB yield by *C. necator*.[4] Monitoring PHB accumulation under different cultural conditions can produce useful data to optimize the design and management of an efficient fermentation process.

Traditional methods for PHB quantification include UV spectrophotometry, gas chromatography/mass spectrometry, and high-performance liquid chromatography. However, data derived from these techniques only provide average information at the population level and mask the heterogeneity among individual cells. Accurate characterization of samples with high cellular heterogeneity may only be achieved by analyzing single cells. Therefore, rapid, convenient, and reliable methods for quantifying PHB content in individual, live cells must be developed to understand the regulation of PHB biosynthesis. Gelder et al.[5] and Hermelink et al.[6] found that confocal Raman spectroscopy can be used to determine PHB content in microorganisms. Raman spectroscopy is especially suitable for monitoring the PHB fermentation process, as it requires only small sample volumes and minimal sample preparation; a single Raman spectrum provides multidimensional information on the chemical composition of individual bacterial cells such as proteins, lipids, and nucleic acids, as well as strain-specific secondary metabolites such as PHB, reflecting cellular metabolic activities and physiological states. The traditional confocal Raman microscopy requires target cell immobilization on a substrate by physical or chemical approaches, which may alter the cellular physiological state. Laser tweezers Raman spectroscopy (LTRS) combines optical trapping and Raman spectroscopy to enable the manipulation and spectroscopic analysis of single, live, and moving cells in a solution.[7] Optical trapping holds the

*Address all correspondence to: Guiwen Wang, E-mail: wguiwen@gxas.cn

1083-3668/2016/$25.00

cell at the focus of the excitation laser, which permits optimum excitation and collection of Raman scattering. In addition, levitating the cell above the cover plate effectively reduces fluorescence and stray scattering interference from the cover slip.[8] Although some degree of photodamage to the living cells may be caused by the trapping bean, this effect can be decreased by selecting near-infrared laser wavelengths, since biological samples usually have small absorption at near-infrared wavelengths.[9] LTRS has been used to study cell dynamics at the single-cell level in different biological systems, such as germination of bacterial spores,[10,11] intracellular ethanol accumulation in yeast cells,[12] and carotenoid synthesis in the yeast *Rhodotorula gulutinis*.[13]

In this study, we applied LTRS to monitor the bacterial growth behavior and PHB production during batch cultivation. We cultured *C. necator* at various carbon-to-nitrogen (C/N) molar ratios and recorded the Raman spectra of individual cells. Dynamic changes in the contents of PHB, nucleic acids, and proteins in *C. necator* cells during fermentation were inferred from the spectral data. Single-cell Raman spectroscopy can provide additional information on the fermentation process, such as the heterogeneity of cellular metabolic activity and the distribution characteristics of bacterial cells with different PHB-producing abilities in a population.

2 Materials and Methods

2.1 *Strain and Culture Medium*

C. necator H16 strain was used in this work.

Agar plate medium contained the following: 10 g/L yeast extract, 10 g/L trypton, 5 g/L beef extract, 5 g/L NaCl, and 20 g/L agar, pH 7.0. Seed medium consisted of the same composition as the plate medium except agar.

Liquid fermentation medium was composed of the following: 20 g/L fructose, 9 g/L $Na_2HPO_4 \cdot 7H_2O$, 1.5 g/L KH_2PO_4, 0.2 g/L $MgSO_4 \cdot 7H_2O$, 0.002 g/L $CaCl_2 \cdot 2H_2O$, 0.5 g/L $NaHCO_3$, 0.005 g/L ammonium ferric citrate, and 1 mL of trace element solution. To investigate the effect of C/N ratio on PHB production, ammonium sulfate was added as a nitrogen source at final concentrations of 0.5, 1.0, 2.0, 4.0, and 6.0 g/L. The trace element solution contained the following: 0.2 g/L $CoCl_2 \cdot 6H_2O$, 0.1 g/L $ZnSO_4 \cdot 7H_2O$, 0.03 g/L $MnCl_2 \cdot 4H_2O$, 0.03 g/L $NaMoO_4 \cdot 2H_2O$, 0.02 g/L $NiCl_2 \cdot 6H_2O$, 0.01 g/L $CuSO_4 \cdot 5H_2O$, 0.02 g/L $FeSO_4 \cdot 7H_2O$, and 0.3 g/L H_3BO_3.

2.2 *Bacterial Culture and Sampling*

Single colonies of *C. necator* from the agar plate were inoculated into 150-mL shake flasks containing 50 mL of seed medium, and then cultivated at 28°C with shaking at 200 rpm for 36 h. The preculture was transferred into 250-mL shake flasks containing 80 mL of fermentation culture medium, and then incubated at 28°C and 200 rpm for 72 h. A 2-mL sample was withdrawn from the culture broth in 3 or 6 h intervals. Each sample was divided into two portions: 1.5 mL for measuring cellular density and 0.5 mL for collecting Raman spectra.

2.3 *Analytical Methods*

Cell growth was monitored by measuring the absorbance of the culture broth at 600 nm on a Beckman DU800S after suitable dilution with 0.9% NaCl. The fructose concentration in the culture broth was estimated through the dinitrosalicylic acid reagent method.[14] Berthlot reaction was used to determine residual ammonia nitrogen concentration.[15]

2.4 *Experimental Setup and Raman Measurements*

Details of the LTRS method have been published elsewhere.[16] In brief, a laser beam from a wavelength-stabilized diode laser (780 nm, 500 mW, TEC300, Sacher Lasertechnik Group, Marburg, Germany) was circularized with a pair of anamorphic prisms, spatially filtered, and then introduced into an inverted differential interference contrast microscope (TE2000U, Nikon, Kanagawa, Japan). The equipped high numerical aperture objective (100×, N.A. = 1.30) was used to focus the laser beam forming an optical trap. The same laser beam was used as the excitation source. The Raman scattering light from a single cell was collected with the same objective, focused onto the entrance slit of an imaging spectrograph, and then recorded with a wind-cooled (−70°C) charge-coupled detector (PIXIS 400BR, Princeton Instruments, Trenton). The spectral resolution of the Raman system was ~6 cm^{-1}. A polystyrene bead of 2.0 μm in diameter suspended in water was used to calibrate the LTRS.

The culture broth was diluted 3000 fold with sterile water and loaded into the hole of the sample holder, which was then sealed with a cover slip. A single bacterial cell was captured by the laser beam and levitated 5 μm above the quartz cover slip to reduce the florescence background from the substrate. The Raman spectrum of the trapped cell was acquired with a 45-mW laser power and 60-s exposure time. The background spectrum without a bacterial cell in the trap was recorded under the same acquisition conditions. The Raman spectra of 50 cells and five background spectra were collected for each sample. All Raman measurements were performed at room temperature (24°C).

2.5 *Raman Data Analysis*

Raw spectral data were saved in ASCII format and imported into Visual Basic 6.0 for data analysis. Background subtraction and response function calibration were conducted as follows: $S_{act}(v) = [S_{acq}(v) - S_{bg}(v)]/R(v)$, where $S_{act}(v)$ is the actual spectrum of a single cell, $S_{bg}(v)$ is the background spectrum, $S_{acq}(v)$ is the raw spectrum acquired by LTRS, and $R(v)$ is the response function of the instrument. A Savitzky–Golay smoothing filter with a window width of nine points was used to remove the noise, and a baseline calibration was performed by using the polynomial fitting method.[17]

3 Results and Discussion

3.1 *Raman Spectra of Cupriavidus necator Cells and Pure Poly(3-Hydroxybutyrate)*

In this study, the PHB production inside *C. necator* cells was monitored through LTRS. All Raman-active molecules, including PHB and other biological macromolecules, contribute to the spectra of bacterial cells, resulting in an overlap of various signals. Therefore, a detailed comparison of the bacterial spectra and the reference spectrum of pure PHB is necessary. Figure 1 shows the Raman spectra of pure PHB (curve D) and bacterial samples cultured at 0 h (curve B) and 20 h (curve A) during fermentation. The differentiated spectrum (curve C) between the spectra of the two bacterial samples above-mentioned

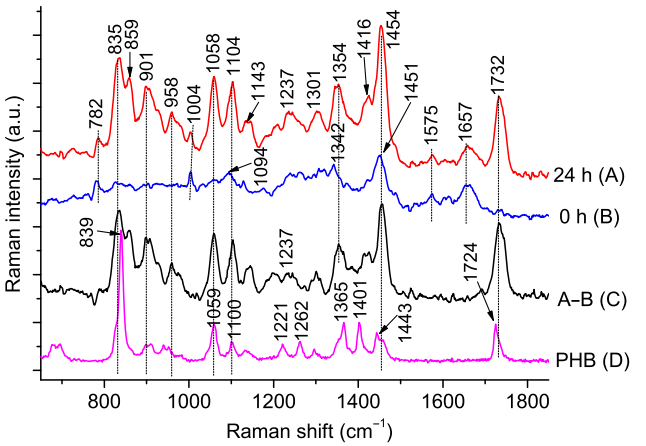

Fig. 1 Raman spectra of *C. necator* cultured for 24 h (curve A) and 0 h (curve B); curve C represents the differentiated spectrum between A and B; and the reference Raman spectrum of PHB is presented by curve D.

(curve A minus curve B) was calculated. As indicated by the reference spectrum of pure PHB, the major peaks of PHB were located at 835, 901, 1058, 1104, 1354, 1456, and 1732 cm^{-1}[15]. Among these Raman bands, the 1732-cm^{-1} characteristic band, which was assigned to a $\gamma(C=O)$ stretching vibration, indicated a strong signal with no peaks from other intracellular components as observed around this region. Hence, this peak was used to evaluate the relative PHB content in *C. necator* cells. Apart from the above bands originating from PHB, bands associated with nucleic acids (located at 725, 782, and 1575 cm^{-1})[18–20] and proteins (located at 1004 and 1657 cm^{-1})[18,20] were observed in the Raman spectra of *C. necator* cells. These bands could provide information on the metabolic activity of individual bacterial cells.

3.2 *Kinetics of Poly(3-Hydroxybutyrate) Fermentation in Cupriavidus necator Cells Cultivated at Various Carbon-to-Nitrogen Ratios*

Unlike carbon source, nitrogen source is not used as a substrate for PHB production in *C. necator* cells. However, nitrogen as an essential nutrient for bacterial growth exerts an indirect but significant influence on PHB biosynthesis. Suitable C/N ratio is also important for effective PHB production.[21] In this study, the time-dependent cellular growth, substrate consumption, and PHB formation in *C. necator* cultivated at various initial C/N ratios were monitored using LTRS and other conventional analytic approaches (Fig. 2). C/N molar ratios of 29.3 to 2.4 were obtained by varying the ammonium sulfate concentration from 0.5 to 6.0 g/L while fixing fructose at 20 g/L. Figure 2(a) illustrates the influence of different C/N ratios on *C. necator* growth, which was measured as optical density at 600 nm. The final bacterial cellular density increased as the initial ammonium sulfate concentrations increased from 0.5 to 2.0 g/L (corresponding to C/N ratios of 29.3 to 7.3). By contrast, the final cellular density decreased when the initial ammonium sulfate concentrations were further increased to 4.0 and 6.0 g/L (corresponding to C/N ratios of 3.7 and 2.4, respectively). This result suggests that a moderate concentration of nitrogen source favors *C. necator* growth, whereas too low or too high concentrations can negatively affect microorganism growth.

The nitrogen source in the culture broth was completely consumed after 9 to 30 h of cultivation at initial C/N ratios of 29.3 to 7.3. However, 46% and 72% of ammonium sulfate were not

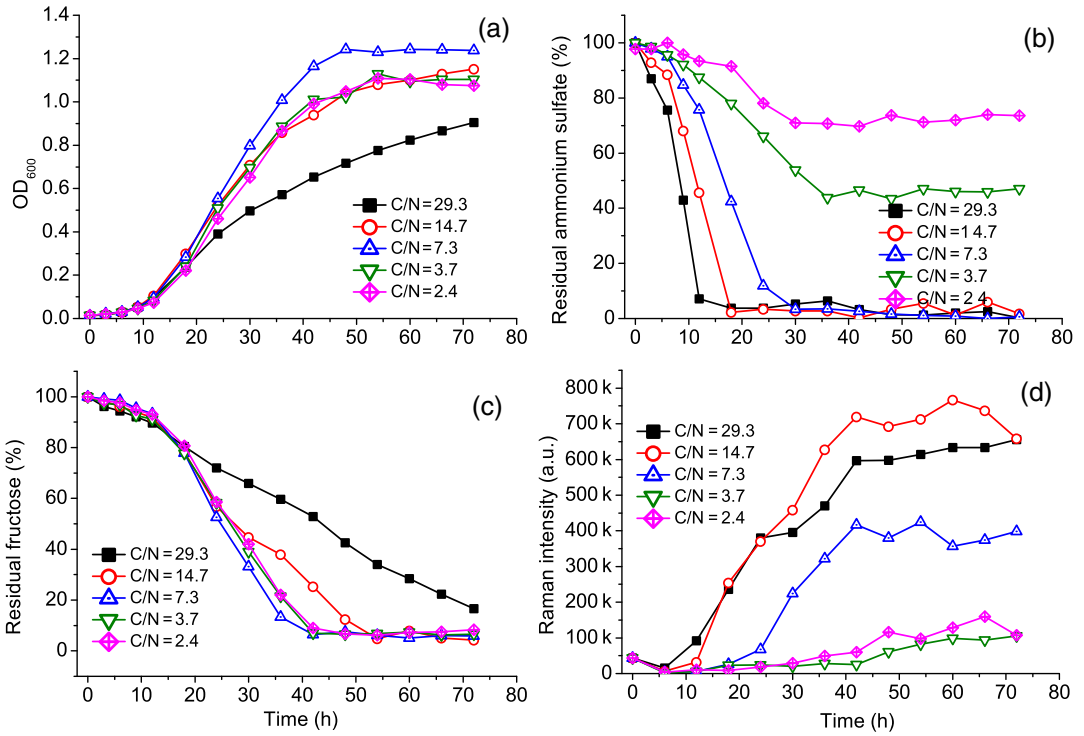

Fig. 2 Time course of PHB fermentation in *C. necator* cells at various initial C/N ratios. (a) Growth of *C. necator*, (b) residual ammonia sulfate, (c) residual fructose, and (d) intensities of Raman band at 1732 cm^{-1}.

utilized and remained in the final culture medium at initial C/N ratios of 3.7 and 2.4, respectively [Fig. 2(b)]. The utilization of carbon source was also influenced by the initial C/N ratio [Fig. 2(c)]. The fructose was metabolized from 42 to 54 h within the C/N ratio of 14.7 to 2.4 but was incompletely consumed until the end of fermentation (72 h) at a C/N ratio of 29.3.

As described above, the intensity of the Raman band at 1732 cm^{-1} can be used to measure PHB content in bacterial cells. Figure 2(d) depicts the time-dependent changes in the band intensity at 1732 cm^{-1}; thus, the relative content of PHB in *C. necator* cells during cultivation at various C/N ratios. For each sample, the Raman spectra of 50 randomly selected individual cells were acquired and their averages were calculated. The band intensity at 1732 cm^{-1} was plotted against its corresponding sampling time. Figure 2(d) shows that the 1732-cm^{-1} band intensity and the PHB accumulation trajectories can be divided into two types: (1) nitrogen-limiting cultivation when the initial C/N ratio ranged from 29.3 to 7.3 and the nitrogen source was depleted during fermentation and (2) balanced growth when the initial C/N ratio was at or below 3.7 and the residual nitrogen source existed in the final culture medium. Under nitrogen-limiting conditions, PHB biosynthesis was triggered when the nitrogen source in the broth was consumed and decreased to a certain suboptimal level. Afterward, the PHB was accumulated dramatically and continuously until the exhaustion of the carbon source. However, under balanced growth conditions, carbon was utilized mainly for cellular growth rather than PHB production because the nitrogen supply was sufficient throughout the cultivation period. Small amounts of PHB polymerization were detected during the late exponential phase and stationary phase probably because of the slight limitation of oxygen or other nutrients.

3.3 *Dynamic Changes in Nucleic Acid and Protein Content Inside Cupriavidus necator Cells During Cultivation*

Nitrogen source plays a vital role in nucleic acid and protein metabolism. Thus, it affects the distribution of carbon flux on cellular growth and PHB accumulation. Tracing the changes in nucleic acid and protein content within *C. necator* cells will enrich our understanding of the regulation of PHB biosynthesis. Figure 3 shows the dynamic changes in intensities of the Raman bands specific to proteins and nucleic acids. The Raman peak at 1657 cm^{-1} was attributed to protein amide I band, and its intensity indicated protein abundance in cells. At relatively high C/N ratios (29.3 to 7.3), the 1657-cm^{-1} band intensity rapidly increased to a high level in a short period after inoculation (6 to 24 h) and then continuously decreased to the lowest value (~50% of the initial intensity). However, at low C/N ratios (3.7 and 2.4), the 1657-cm^{-1} peak intensity elevated to the highest value during the first 6 h of cultivation and was maintained in such a high level throughout the remaining period [Fig. 3(a)]. The Raman band at 782 cm^{-1} is associated with nucleic acids consisting of DNA and RNA. RNA is considerably more abundant than DNA in a prokaryotic cell;[22] thus, the 782-cm^{-1} peak intensity is mainly related to the RNA content of bacterial cells. Figure 3(b) illustrates that the intensities of the 782-cm^{-1} band exhibited a similar trend to those of the 1657-cm^{-1} band, i.e., the band intensity at relatively high C/N ratios rapidly increased and then declined, whereas the 782-cm^{-1} peak intensity at low C/N ratios maintained a high level throughout the fermentation period except at the early growth phase.

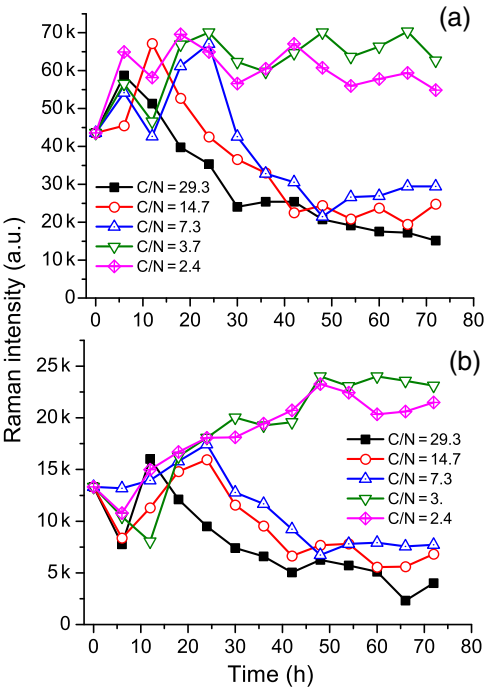

Fig. 3 Time course of intensities of Raman bands at (a) 1657 cm^{-1} and (b) 782 cm^{-1} from *C. necator*.

To elucidate the relationship among the metabolic activities of PHB, proteins, and nucleic acids, we calculated the correlations between the Raman bands associated with these substances in bacterial cells cultivated at initial C/N ratios of 29.3 to 2.4 and sampled at 0 to 72 h (Fig. 4). A linear relationship was observed between the intensities of the 782- and 1657-cm^{-1} bands with a correlation coefficient of 0.85 [Fig. 4(a)]. This finding implies that the protein content positively correlated with the RNA level in *C. necator* cells. The reason behind this correlation is that ribosomal RNA, which constitutes 80% to 85% of total RNA, forms structural and functional components of ribosomes that serve as the subcellular units responsible for protein synthesis. Therefore, the intensity of the 782- or 1657-cm^{-1} band may indicate the metabolic activity involved in cellular growth. Furthermore, the 1732-cm^{-1} peak intensities plotted against the 1657-cm^{-1} peak intensities showed a linear relationship with a correlation coefficient of −0.86 [Fig. 4(b)]. This result suggests that the PHB production and protein content negatively correlated in individual cells. After completing a comprehensive analysis of the data from Figs. 2, 3, and 4, the changes in PHB, nucleic acid, and protein contents inside *C. necator* cells can be explained as follows. On the one hand, when the bacterial cells were cultured under balanced growth conditions (low C/N ratios), the carbon source was mostly used for cellular growth rather than PHB production. On the other hand, under nitrogen-limiting growth conditions, the syntheses of proteins and/or nucleic acids were blocked, and cellular growth was inhibited. This phenomenon triggered the shift of carbon flux from the tricarboxylic acid cycle to the PHB biosynthetic pathway.

3.4 *Single-Cell Analysis of Poly(3-Hydroxybutyrate) Production in Cupriavidus necator*

Current knowledge on the growth characteristics of *C. necator* and conditions of PHB synthesis was mostly obtained by

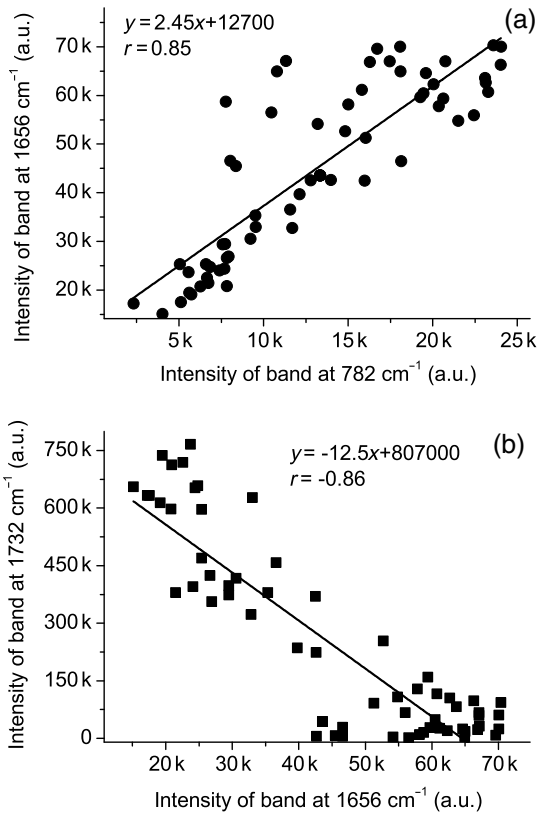

Fig. 4 Correlation between the intensities of Raman bands at (a) 1657 and 782 cm^{-1} and at (b) 1732 and 1657 cm^{-1}.

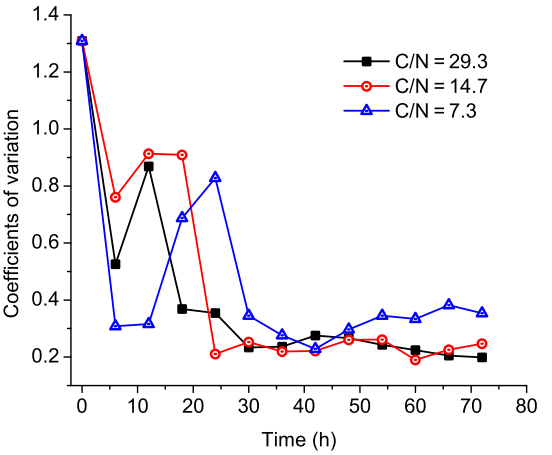

Fig. 5 Time-dependent changes in CVs for the 1732-cm^{-1} Raman band intensity of *C. necator* cells cultivated at C/N ratios of 29.3, 14.7, and 7.3.

monitoring fermentation parameters with conventional chemical analytic methods. However, these methods only provide average values over the population of a culture consisting of millions of cells. In many cases, individual cells in a population, even if derived from the same clone, show different responses to environmental changes because of population heterogeneity. Hence, single-cell-based analytic techniques are required to reveal this heterogeneity in the responses of individual cells. In this work, we employed LTRS to assess the PHB levels in individual cells by measuring the Raman scattering intensities of PHB-associated bands and evaluated the variation in PHB levels per cell over 50 single cells of *C. necator* at varying time points of the batch growth. Figure 5 presents the time-dependent changes in the coefficients of variation (CVs, standard deviation/mean) of 1732 cm^{-1} Raman band intensities of bacterial cells cultivated within the C/N ratio of 29.3 to 7.3. Under all the culture conditions, the highest CV values (above 1.30) were observed at the beginning of the cultivation (0 h), suggesting an extremely inhomogeous nature of the PHB content among the individual cells of the inoculums. During the lag phase, the PHB that accumulated during the preculture degraded in most of the cells within the microbial populations exposed to relatively rich nitrogen supply in the fresh fermentation medium. This phenomenon resulted in homogeneous, low PHB levels inside the cells and, thus, decreased the CV to low values (0.31 to 0.76). The second highest CV values (0.83 to 0.91) were observed at the early stage of PHB synthesis (12 to 24 h), when the residual nitrogen source in the culture broth was consumed to a suboptimal concentration. Bacterial cells at varying stages in their life cycle respond differently to nitrogen limitation stress. Thus, the asynchronous behavior of the individual cells in the populations caused a great heterogeneity in PHB accumulation, i.e., some of the cells initiated PHB accumulation instantaneously, whereas the others needed a relatively long preparation time for PHB biosynthesis. After the middle exponential phase of growth, most cells initiated PHB synthesis and PHB content variation; thus, the CV value drastically decreased to low levels (0.20 to 0.38) and was maintained at such a level for the remaining cultivation period. The above results show that LTRS method can reveal the heterogeneity within a *C. necator* cell population under dynamic process conditions and give us a more comprehensive view of the physiological state of a growing microbial population. Because the phenotypic heterogeneity has important practical consequences for the productivity and stability of industrial fermentations,[23] integrating such information with microbial population characteristics measured via conventional analysis methods will ultimately allow one to develop, control, and enhance microbial performances in PHB fermentation.

In PHB fermentation, each cell contributes to the final product yield, although dead, inactive, or weakly active cells limit this productivity. Therefore, detailed information on single-cell behavior within a cell population will be beneficial to the evaluation and control of such processes. Figure 6 shows the violin plots representing the PHB content distribution of single cells cultured at an initial C/N ratio of 29.3. Violin plots are similar to box plots, except that they also show the probability density of the data at different values.[24] The white dots in Fig. 6 indicate the median, allowing quick comparisons of average PHB levels among multiple bacterial samples, whereas the black bars indicate the first and third quartiles. The surrounding violin shell consists of a mirrored local kernel density estimation that graphically shows the distributional characteristics of PHB content at the single-cell level within each sample. The bacterial cell populations sampled at certain cultivation stages (e.g., at 12, 36, 66, or 72 h) were evidently composed of two or three subpopulations on the basis of PHB abundance in individual cells. Numerous factors, including cell cycle phases, individual cell age, microenvironmental conditions, and mutations,[25] can cause this multimodal distributions of metabolite content in individual cells within a population. Further investigations can be conducted in the future by combining LTRS with other

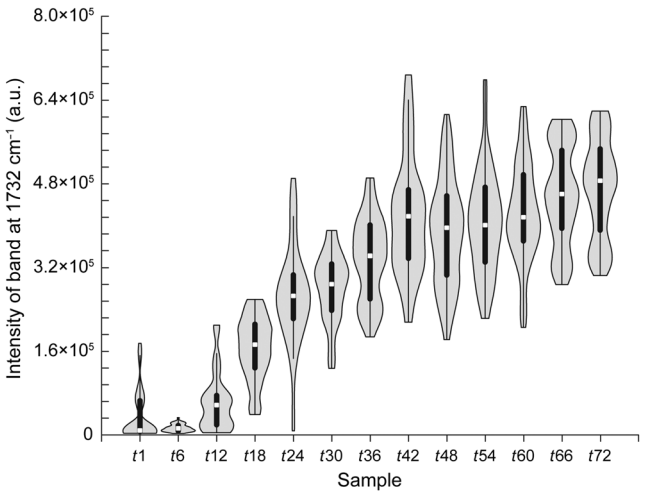

Fig. 6 Violin plots for the distributions of 1732-cm^{-1} Raman band intensities of *C. necator* cultured for different times at an initial C/N ratio of 29.3. Raman spectra of ~50 individual cells were recorded for each sample. In the *X*-axis, the categorical variables of *t*1 to *t*72 correspond to bacterial samples taken at time points of 0 to 72 h, respectively.

sophisticated and high-throughput techniques, such as transcriptomic or proteomic methods, to disintegrate microbial populations and to understand their innate molecular heterogeneity. For instance, LTRS may be used to sort the subpopulations of interest on the basis of PHB content in individual cells, and then the gene expression profiles of the sorted subpopulations may be obtained through transcriptomic or proteomic analyses. Such a strategy may help identify the nature of these subpopulations.

4 Conclusions

This work investigated the effect of various C/N ratios on PHB production in *C. necator* at the population and single-cell levels. For the single-cell investigation, LTRS was used to trap single cells and acquire their Raman spectra. The Raman band intensities at 1732, 1657, and 782 cm^{-1} were used to assess PHB, nucleic acid, and protein contents in bacterial cells, respectively. When the bacterial cells were cultured under balanced growth conditions (low C/N ratios), the biosynthetic activities of nucleic acids and proteins were maintained at high levels, and only small amounts of PHB were produced throughout the fermentation period. However, the syntheses of nucleic acids and proteins were blocked, and PHB was accumulated in massive amounts inside the microbial cells during the batch cultivation under nitrogen-limiting growth conditions (high C/N ratios). Single-cell analysis provided additional insights into the heterogeneity of cellular metabolic activity and the distribution characteristic of the PHB-producing ability of individual cells in a population. A relatively high heterogeneity in PHB level was observed at the beginning of the cultivation and the early stage of PHB synthesis. In addition, bacterial cells in populations at certain cultivation stages (e.g., at 12, 36, 66, or 72 h) can be divided into two or three subpopulations on the basis of their PHB abundance. We conclude that LTRS, as a reliable single-cell analysis tool, can provide a more comprehensive view of PHB fermentation compared with conventional PHB quantification approaches.

Acknowledgments

This work was supported by the National Natural Science Foundation of China (Nos. 11264004 and 31460035) and the Guangxi Natural Science Foundation (Nos. 2012GXNSFCA053001, 2013GXNSFAA019043, and 2014GXNSFAA118193).

References

1. J. Choi and S. Y. Lee, "Factors affecting the economics of polyhydroxyalkanoate production by bacterial fermentation," *Appl. Microbiol. Biotechnol.* **51**(1), 13–21 (1999).
2. P. Raje and A. K. Srivastava, "Updated mathematical model and fed-batch strategies for poly-beta-hydroxybutyrate (PHB) production by *Alcaligenes eutrophus*," *Bioresour. Technol.* **64**(3), 185–192 (1998).
3. K. Kuchta et al., "Studies on the influence of phasins on accumulation and degradation of PHB and nanostructure of PHB granules in *Ralstonia eutropha* H16," *Biomacromolecules* **8**(2), 657–662 (2007).
4. G. C. Du et al., "Effects of environmental conditions on cell growth and poly-beta-hydroxybutyrate accumulation in *Alcaligenes eutrophus*," *World J. Microbiol. Biotechnol.* **16**(1), 9–13 (2000).
5. J. D. Gelder et al., "Monitoring poly(3-hydroxybutyrate) production in *Cupriavidus necator* DSM 428 (H16) with Raman spectroscopy," *Anal. Chem.* **80**(6), 2155–2160 (2008).
6. A. Hermelink, M. Stammler, and D. Naumann, "Observation of content and heterogeneity of poly-beta-hydroxybutyric acid (PHB) in *Legionella bozemanii* by vibrational spectroscopy," *Analyst* **136**(6), 1129–1133 (2011).
7. J. W. Chan, "Recent advances in laser tweezers Raman spectroscopy (LTRS) for label-free analysis of single cells," *J. Biophotonics* **6**(1), 36–48 (2013).
8. C. Xie et al., "Study of dynamical process of heat denaturation in optically trapped single microorganisms by near-infrared Raman spectroscopy," *J. Appl. Phys.* **94**(9), 6138 (2003).
9. C. Xie et al., "Real-time Raman spectroscopy of optically trapped living cells and organelles," *Opt. Express* **12**(25), 6208–6214 (2004).
10. G. W. Wang et al., "Kinetics of germination of wet-heat-treated individual spores of *Bacillus* species, monitored by Raman spectroscopy and differential interference contrast microscopy," *Appl. Environ. Microbiol.* **77**(10), 3368–3379 (2011).
11. G. W. Wang et al., "Germination of individual *Bacillus subtilis* spores with alterations in the GerD and SpoVA proteins, which are important in spore germination," *J. Bacteriol.* **193**(9), 2301–2311 (2011).
12. L. Peng et al., "Intracellular ethanol accumulation in yeast cells during aerobic fermentation: a Raman spectroscopic exploration," *Lett. Appl. Microbiol.* **51**(6), 632–638 (2010).
13. Z. H. Tao et al., "Monitoring and rapid quantification of total carotenoids in *Rhodotorula glutinis* cells using laser tweezers Raman spectroscopy," *FEMS Microbiol. Lett.* **314**(1), 42–48 (2011).
14. G. L. Miller, "Dinitrosalicylic acid reagent for determination of reducing sugar," *Anal. Chem.* **31**, 426–428 (1959).
15. F. Srienc, B. Arnold, and J. E. Bailey, "Characterization of intracellular accumulation of poly-beta-hydroxybutyrate (PHB) in individual cells of *Alcaligenes eutrophus* H16 by flow cytometry," *Biotechnol. Bioeng.* **26**(8), 982–987 (1984).
16. C. Xie, M. A. Dinno, and Y. Q. Li, "Near-infrared Raman spectroscopy of single optically trapped biological cells," *Opt. Lett.* **27**(4), 249–251 (2002).
17. B. D. Beier and A. J. Berger, "Method for automated background subtraction from Raman spectra containing known contaminants," *Analyst* **134**(6), 1198–1202 (2009).
18. Z. Movasaghi, S. Rehman, and I. U. Rehman, "Raman spectroscopy of biological tissues," *Appl. Spectrosc. Rev.* **42**(5), 493–541 (2007).
19. J. De Gelder et al., "Reference database of Raman spectra of biological molecules," *J. Raman Spectrosc.* **38**(9), 1133–1147 (2007).
20. I. Notingher et al., "Spectroscopic study of human lung epithelial cells (A549) in culture: living cells versus dead cells," *Biopolymers* **72**(4), 230–240 (2003).
21. A. Mulchandani, J. Luong, and C. Groom, "Substrate inhibition kinetics for microbial growth and synthesis of poly-β-hydroxybutyric acid by

Alcaligenes eutrophus ATCC 17697," *Appl. Microbiol. Biotechnol.* **30**(1), 11–17 (1989).
22. M. T. Madigan et al., *Brock Biology of Microorganisms*, 14th ed., Benjamin Cummings, San Francisco, California (2014).
23. F. Delvigne and P. Goffin, "Microbial heterogeneity affects bioprocess robustness: dynamic single-cell analysis contributes to understanding of microbial populations," *Biotechnol. J.* **9**(1), 61–72 (2014).
24. J. L. Hintze and R. D. Nelson, "Violin plots: a box plot-density trace synergism," *Am. Stat.* **52**(2), 181–184 (1998).
25. S. Muller, H. Harms, and T. Bley, "Origin and analysis of microbial population heterogeneity in bioprocesses," *Curr. Opin. Biotechnol.* **21**(1), 100–113 (2010).

Zhanhua Tao is an associate researcher at Guangxi Academy of Sciences. He received his PhD in biochemistry and molecular biology from Harbin Medical University in 2006. His current research interests include laser science, spectroscopy, and microscopy for biomedical application.

Pengfei Zhang obtained his PhD in optics from Shanghai Institute of Optics and Fine Mechanics in 2008. In 2009, he joined East Carolina University as a postdoc and worked on laser tweezers and Raman spectroscopy. In 2012, he joined Los Alamos National Laboratory as a postdoctoral research associate, and his research focused on advanced light microscopy and single molecule spectroscopy. He joined Washington University in St. Louis in 2016 as a research associate and is working on photoacoustic imaging.

Zhaojun Qin received his MSc degree from Guangxi Normal University in 2013 and is a lecturer of physics at Guangxi University, Xingjian College of Science and Liberal Arts.

Yong-Qing Li is a professor of physics at East Carolina University. He obtained his PhD in optics from Shanghai Institute of Optics and Fine Mechanics, Chinese Academy of Sciences in 1989. His research interests include biophysics of single bacterial spores, optical tweezers and Raman spectroscopy, confocal Raman imaging, interactions between light and biological systems, quantum optics, and atomic physics.

Guiwen Wang is a professor at Guangxi Academy of Sciences. His research focuses on the biomedical application of Raman spectroscopy, biophysics of single microbial cells, microbial physiology, and applied microbiology.